Fully Differential Study of Capture with Vibrational Dissociation in $p + H_2$ Collisions

B. R. Lamichhane,[1] T. Arthanayaka,[1] J. Remolina,[1] A. Hasan,[1,2] M. F. Ciappina,[3] F. Navarrete,[4,5] R. O. Barrachina,[4,5] R. A. Lomsadze,[1,6] and M. Schulz[1]

[1]*Department of Physics and LAMOR, Missouri University of Science & Technology, Rolla, Missouri 65409, USA*
[2]*Department of Physics, UAE University, P.O. Box 15551, Al Ain, Abu Dhabi, United Arab Emirates*
[3]*Institute of Physics of the ASCR, ELI-Beamlines, Na Slovance 2, 182 21 Prague, Czech Republic*
[4]*Centro Atómico Bariloche and Instituto Balseiro (Comisión Nacional de Energía Atómica and Universidad. Nacional. de Cuyo), Bariloche, 8400 Río Negro, Argentina*
[5]*Consejo Nacional de Investigaciones Científicas y Técnicas (CONICET), 2290 Caba, Argentina*
[6]*Tbilisi State University, Tbilisi 0179, Georgia*

(Received 23 February 2017; revised manuscript received 12 May 2017; published 24 August 2017)

We have measured fully differential cross sections for electron capture in 75 keV $p + H_2$ collisions with subsequent dissociation of the intermediate molecular H_2^+ ion by vibrational excitation using different projectile coherence lengths. Data were obtained for two molecular orientations as a function of projectile scattering angle. Two types of interference, single- and molecular two-center interference, were identified. The two-center interference structure is phase shifted by π compared to what we expected. Furthermore, the presence of projectile coherence effects could be reconfirmed.

DOI: 10.1103/PhysRevLett.119.083402

One of the most important goals of studies on atomic fragmentation processes is to advance our understanding of the few-body problem (FBP) e.g., Refs. [1,2]. The essence of the FBP is that the Schrödinger equation is not analytically solvable for more than two mutually interacting particles even when the underlying forces are precisely known. Therefore, elaborate numerical models have to be developed for its theoretical analysis, and the approximations entering in these models need to be tested by detailed experimental data. To this end, numerous kinematically complete experiments on atomic fragmentation processes induced by charged particle impact have been performed [3,4].

The most basic fragmentation process in ion-atom collisions is single target ionization. For this process, the primary interaction occurs between the projectile and a target electron. In fact, it is remarkable how well the basic features observed in measured cross sections can qualitatively be reproduced by theories that ignore the interaction between the nuclei (NN interaction) in the collision, especially for small perturbation parameters (projectile charge to speed ratio $\eta = Q_p/v_p$), e.g., Refs. [5–7]. Nevertheless, in order to obtain good quantitative agreement it is important to account for the NN interaction, especially at large η, e.g., Refs. [8,9]. However, this interaction usually only plays a "passive" role in inelastic processes in so far as it does not directly cause target fragmentation by actively triggering electronic transitions. Such a process is not impossible; for example, the projectile could undergo a head-on collision with the target nucleus causing it to recoil at such a large speed that it cannot be followed by the electron. But the cross section for this mechanism is negligible.

For molecular targets, the role of the NN interaction in the collision dynamics can be qualitatively different from atomic targets because not only are the electrons bound inside the molecule, but the atoms are also bound to each other. Therefore, additional inelastic channels like dissociation are opened for molecular targets. Dissociation can proceed through an electronic transition to a repulsive state, but it can also be caused by vibrational excitation of the nuclear motion (e.g., Ref. [10]), in which the NN interaction can play an active role. Fully differential studies of dissociative processes induced by charged particle impact are rare. Three kinematically complete experiments on dissociative capture of H_2 or H_2^+, two of them using reversed kinematics, were performed for atom or ion impact [11–13]. In two of them, dissociation by electronic transitions was investigated. In the other, the interest was focused on the nuclear wave functions of the molecule for different vibrational states and no fully differential cross sections (FDCS) were reported. FDCS for dissociation of H_2 by vibrational excitation, accompanied by ionization, were measured for electron impact [14]. To the best of our knowledge, no measured FDCS for dissociative processes through vibrational excitation induced by ion impact have been reported yet.

Another important aspect of collisions with molecular targets that was discussed in recent years is a potential influence of projectile coherence effects on the collision dynamics (e.g., Refs. [15–20]). Experiments were performed for different transverse coherence lengths of the projectiles by placing a collimating slit at varying distances from the target. Interference structures were present for large coherence lengths, but (nearly) absent for small coherence

lengths. Earlier, a similar dependence of the interference visibility on the coherence length was studied for Ar atoms interacting with a standing light wave [21]. Later, such effects were observed for atomic targets [22–24]. In another recent study, performed for a collision system corresponding to small η, no significant differences in the cross sections for varying coherence lengths were found [25]. However, there the coherence lengths were orders of magnitude larger than the small coherence length studied in Ref. [22] for a very similar η and larger than the size of the target atom. Therefore, for small η the role of coherence effects is not conclusively settled yet and further experimental and theoretical work is needed. In contrast, for η close to unity by now there is an extensive literature on experimental and theoretical studies, e.g., Refs. [15–18,20,26,27] supporting the interpretation that scattering cross sections can be significantly affected by the projectile coherence properties. In this regime, experimental studies now enter a phase in which such coherence effects are used as a tool to sensitively investigate the few-body reaction dynamics.

In this Letter, we report the first FDCS for capture accompanied by dissociation of H_2 through vibrational excitation. The data provide additional support for the presence of projectile coherence effects. More importantly, by analyzing the ratios between the FDCS for coherent and incoherent projectiles, interference structures could be investigated very sensitively. Two types of interference, single- and two-center interference, were identified. In the latter, an unexpected phase shift in the interference pattern was observed.

The experiment was performed as follows. A 75 keV proton beam was passed through vertical and horizontal collimating slits with widths of 150 μm. The horizontal slit (y slit) was placed at a distance $L_1 = 50$ cm and the vertical slit (x slit) at a distance $L_2 = 6.5$ cm from the target. These slit geometries correspond to coherence lengths of $\Delta x \approx 1.0$ and $\Delta y \approx 3.3$ a.u., respectively (see Ref. [17] for a detailed analysis of the coherence lengths at different L). After traversing the target region the projectiles were charge-state analyzed by a switching magnet and the neutralized beam component was detected by a two-dimensional position-sensitive multichannel plate detector. From the position information the polar scattering angle θ_p was determined separately for scattering in the x and y directions; i.e., cross sections were recorded for projectiles with a small and a large coherence length simultaneously under identical experimental conditions.

A cold H_2 target beam ($T < 2$ K) was generated with a supersonic gas jet and intersected the projectile beam. This temperature corresponds to thermal energies small compared to rotational and vibrational excitation energies. A capture process in the collision could lead to either an H_2^+ recoil ion or, if accompanied by dissociation, to two molecular fragments, of which at least one must be a proton. The recoil ions were extracted by an electric field of about 50 V/cm and detected by a two-dimensional position sensitive multichannel plate detector, which was set in coincidence with the projectile detector. In the coincidence time spectrum the H_2^+ ions and protons are represented by separate peak structures due to their mass-dependent time of flight. The shape of each peak contains the momentum information in the direction of the extraction field. The other two momentum components are obtained from the position information. The momentum of the undetected molecular fragment is determined by momentum conservation. Finally, the kinetic energy release (KER) in the dissociation was calculated from the momenta of the fragments.

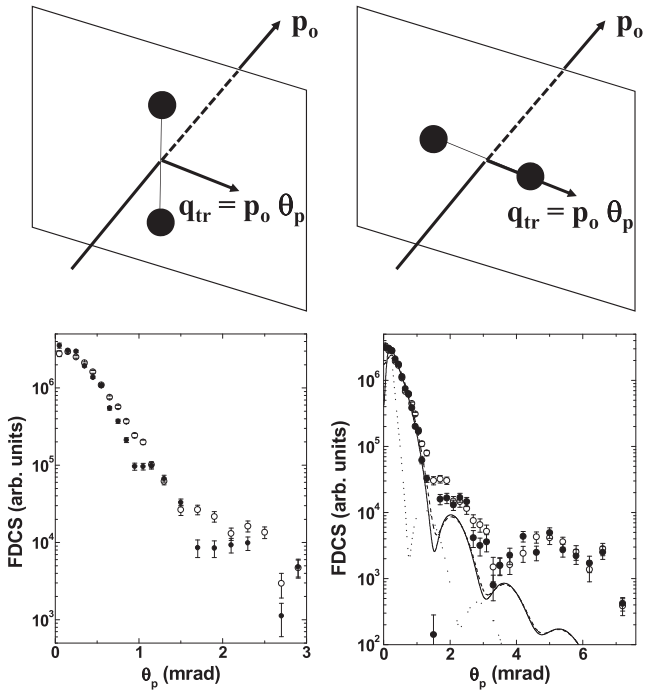

FIG. 1. Fully differential cross sections (lower panels) for dissociative capture leading to KER = 0–2 eV and for the two molecular orientations illustrated in the top panels as a function of scattering angle measured with incoherent (open symbols) and coherent (closed symbols) projectiles. Both molecular orientations are perpendicular to the beam axis, but one (left panels) is also perpendicular to the transverse component of the momentum transfer q_{tr} while the other (right panels) is parallel to q_{tr}. Dotted curve, coherent eikonal calculation with $\delta = 0$ in the two-center interference term; dashed (solid) curves, incoherent (coherent) eikonal calculations with $\delta = \pi$ in the two-center interference term.

FDCS for dissociative capture were extracted for a fixed KER of 0–2 eV and for various fixed molecular orientations as a function of θ_p. Such a small KER selects events in which dissociation is caused by vibrational excitation of the molecule rather than by a transition of the second electron to a repulsive state, e.g., Refs. [10,14]. For each orientation FDCS were obtained for incoherent and coherent projectiles by setting conditions on scattering in the x and y directions, respectively. In Fig. 1, these FDCS are shown for two molecular orientations, illustrated in the top panels of Fig. 1, both of which are perpendicular to the initial projectile beam axis. One orientation (upper left panel) is

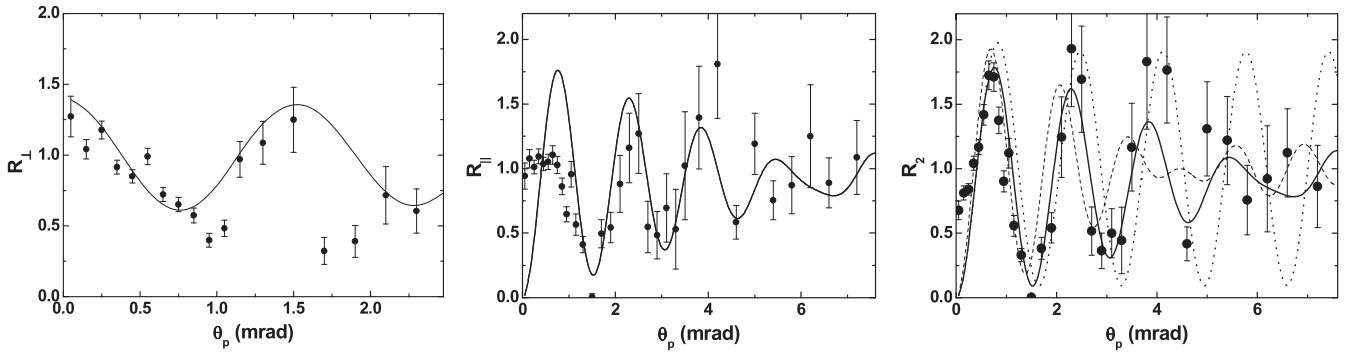

FIG. 2. Left panel: ratios $R_\perp$ between the coherent and incoherent FDCS of Fig. 1 for the perpendicular orientation. The solid curve shows I_1 calculated for $\Delta b = 1.3$ a.u. Center panel: ratios $R_\parallel$ between the coherent and incoherent FDCS of Fig. 1 for the parallel orientation. Right panel: double ratios $R_2 = R_\parallel/R_\perp$. The curves in the center and right panels show the two-center interference term for $\delta = \pi$ and $D = 1.2$ a.u. (dotted curve), averaged over all D assuming equal weights (dashed curve), and averaged over all D with a weight factor decreasing with increasing D (solid curve) (see text).

perpendicular also to the transverse component of the momentum transfer $q_{\rm tr}$ while the second orientation is parallel to $q_{\rm tr}$ (upper right panel). In the following we refer to these orientations as the perpendicular and parallel orientations, respectively. The open (closed) symbols represent the incoherent (coherent) FDCS.

Some differences between the various data sets can be seen. The θ_p dependence of the FDCS for the perpendicular orientation is narrower than the one for the parallel orientation. As a result, statistically significant data could only be obtained up to about 2.5 mrad, while for the parallel orientation this range extends to about 6 mrad. Furthermore, in the coherent data for the perpendicular orientation we observe a structure at small θ_p, which is missing in the incoherent data and in both data sets for the parallel orientation: the coherent FDCS are above the incoherent FDCS for small θ_p, they cross the latter near $\theta_p = 0.3$ mrad, reach a shallow minimum at about $\theta_p =$ 0.9 to 1.0 mrad, and approach the incoherent FDCS again near $\theta_p = 1.2$ mrad. It is not clear whether the two data points below and above 1.75 mrad represent another minimum or just statistical fluctuations.

For the parallel orientation significant differences between the incoherent and coherent data sets are only discernable for $\theta_p > 1.0$ mrad. For this orientation significant structures are found at large θ_p suggesting interference minima at about 1.5 and 3.2 mrad and maxima around 2.2 and possibly at 4.8 mrad. These structures are also present in the incoherent data; however, they are significantly more pronounced in the coherent case as we will illustrate by analyzing the coherent to incoherent cross section ratios.

The oscillations in the FDCS are more prominent in the ratio R between the coherent and incoherent FDCS, which is plotted for the perpendicular orientation ($R_\perp$) in the left panel of Fig. 2. These ratios represent the interference term; however, it is not self-evident what type of interference is reflected by the oscillations. The phase angle in two-center interference is given by $\mathbf{p_{rec}} \cdot \mathbf{D}$, where for a capture process the recoil ion momentum $\mathbf{p_{rec}}$ is equal to $\mathbf{q}$, and $\mathbf{D}$ is the internuclear separation vector in the molecule, e.g., Refs. [12–14]. For the perpendicular orientation this dot product is zero so that here two-center interference cannot lead to any structure in R. We therefore interpret the oscillations observed for the perpendicular orientation as being caused by single-center interference. There, different impact parameters leading to the same scattering angle interfere with each other [24].

A simple model single-center interference term was suggested by Sharma *et al.* [17] as $I_1 = [1 + \alpha\cos(q_{\rm tr}\Delta b)]$, where α accounts for a reduction in visibility of the interference due to incomplete coherence even at the large slit distance and due to the experimental resolution. Δb represents an effective impact parameter range contributing to the dissociation process, which we approximate as being independent of $q_{\rm tr}$. A similar analysis was performed for single capture in energetic p + He collisions [28]. The solid curve in the left panel of Fig. 2 shows a best fit of the single-center interference term to the measured ratios yielding $\alpha = 0.4$ and $\Delta b = 1.3$ a.u. This value of Δb appears to be a reasonable reflection of the effective dimension of the diffracting object. However, because of the approximations entering in this analysis it represents only a crude estimate.

The center panel of Fig. 2 shows the coherent to incoherent FDCS ratios for the parallel orientation $R_\parallel$. As seen already in the FDCS in Fig. 1, $R_\parallel$ is nearly flat up to about 0.8 to 1.0 mrad. However, at larger θ_p, between approximately 1 and 4 mrad, pronounced oscillations are observed, which shows that indeed the structures in the coherent FDCS are significantly more pronounced than in the incoherent FDCS, as mentioned earlier. Both single- and two-center interference can contribute to this orientation so that we expect $R_\parallel$ to be determined by a product of both interference terms $I_1 I_2$. We make the approximation that Δb is the same for the parallel and perpendicular orientations, which is not necessarily the case. With that assumption we obtain the two-center interference term I_2 as the ratio $R_2 = R_\parallel/R_\perp$, which is plotted in the right panel of Fig. 2. In these double ratios the oscillating pattern extends to angles smaller than 1 mrad. The nearly flat

behavior of $R_\parallel$ at small θ_p can now be understood as a compensation between single- and two-center interference. While single-center interference alone would make $R_\parallel$ drop with θ_p increasing from 0, two-center interference alone would make it increase.

A striking feature of the θ_p dependence of R_2 is that there is a minimum at $\theta_p = 0$, while the two-center interference term $I_2 = 1 + \alpha \cos(q_{\mathrm{tr}} D)$ predicts a maximum. This minimum suggests that there is a shift of π in the phase angle of the interference term. The dotted curve in the right panel of Fig. 2 shows the two-center interference term I_2 with a phase shift of π incorporated. Here, we used 1.2 a.u. instead of the equilibrium distance of 1.4 a.u. for D because vibrational dissociation mostly occurs near the inner turning point [14], i.e., at the minimum distance in the Franck-Condon region $D_{\mathrm{min}} \approx 1.2$ a.u. [29]. Reasonably good agreement with R_2 is achieved; however, the calculated interference term appears to be slightly shifted to larger θ_p. This shift is expected because although vibrational dissociation occurs mostly at the inner turning point, the contributions from other D within the Franck-Condon region are not necessarily negligible. We therefore also calculated I_2 averaged over the entire Franck-Condon region. The dashed curve shows this calculation (unrealistically) assuming that all D contribute equally. Now, with increasing θ_p I_2 is increasingly shifted to smaller θ_p. This is not surprising either because the influence of large D on the interference term is now overestimated. The actual distribution of D contributing to vibrational dissociation is not known. However, the comparison between the data and the dotted and dashed curves suggest that the data may be reproducible by some distribution in between the extremes of only a single-valued (at $D = 1.2$ a.u.) and a uniform distribution of D. As an example, the solid curve in the center and right panels shows I_2 averaged over the Franck-Condon region giving each D a weight $f = (3.4 - 2D)^2$, so that $f = 1$ for $D = 1.2$ a.u. and $f = 0.01$ for $D = 1.65$ a.u. (outer turning point). This calculation is in very good agreement with the measured R_2. The deviation seen in $R_\parallel$ at small θ_p is due to the contributions from single-center interference. This shows that our data are consistent with the assumption that vibrational dissociation occurs mostly at the inner turning point and falls off with increasing D, but it does not prove that f represents the correct distribution of D. Most importantly, the data cannot even be remotely reproduced by I_2 for any distribution of D if the phase shift of π is not included, in which case minima and maxima would be reversed compared to the measured data.

It should be noted that even the small KER analyzed here is much larger than typical rotational energies of the molecule (a few meV). Therefore, the axial recoil approximation (ARA) should be valid, meaning that the momentum direction of the detected fragment does reflect, to a good approximation, the molecular orientation at the instance of the collision. This is confirmed by our measured cross sections as a function of the molecular orientation (see Fig. S1 in the Supplemental Material [30]), which exhibit maxima parallel to the projectile direction and a minimum perpendicular to it. If the ARA would be significantly violated this angular dependence would be flat. If the ARA is valid, then without any phase shift a maximum should be observed perpendicular to the projectile direction and minima parallel to it. Therefore, our measured orientation-dependent cross sections further confirm the presence of a π phase shift.

The same phase shift was also reported for dissociative capture [11] and excitation [31] in $H_2^+ + He$ collisions. In both cases the phase shift was explained by a change of symmetry in the electronic state during the transition. However, no phase shift was found in dissociative capture in $p + H_2$ collisions [13,32]. The authors argued that this showed that the dominant dissociation channel was one where the first electron is captured from a symmetric molecular state while the second electron is excited to a molecular ungerade state. On the other hand, based on the symmetry arguments given in Ref. [11] a phase shift of π would be expected in this case. At the same time, a shift of the interference pattern was observed in dissociative ionization by electron impact [14], where no change of symmetry in the electronic state occurs, like in the present data. Nevertheless, the shift of the interference pattern was reproduced by a calculation, in which the interference term is included from first principles [14]. A comprehensive evaluation of these experimental and theoretical results suggests that the two-center interference pattern is not fully understood yet: while two data sets (Refs. [11,31]) are consistent with a π phase shift due to a change in symmetry in the electronic state, three data sets (Refs. [13,14] and the present data) appear to behave opposite to the expectation based on the symmetry of the electronic state. Therefore, apart from the electronic symmetry there appear to be other causes that can lead to a phase shift in the interference term.

We have calculated the FDCS for the parallel orientation using a molecular eikonal approach. This method was described previously and successfully reproduces FDCS for single capture in 75 keV $p + H_2$ collisions [33]. Conceptually, all interactions are accounted for, including the NN interaction, and treated fully quantum mechanically. Since the molecular target wave function is modeled in terms of atomic states, two-center interference is not included directly. Rather, it is incorporated by multiplying the cross sections with the interference term $I_2 = 1 + \cos(q_{\mathrm{tr}} D + \delta)$ (see, e.g., Refs. [33,34]) averaged over the Franck-Condon region using the same weight factor f as for the curve in the right panel of Fig. 2. The projectile coherence properties are accounted for using the method of Sarkadi *et al.* [20], i.e., by describing the projectiles in terms of a Gaussian wave packet, where the width reflects the coherence length.

The dotted curve in the right panel of Fig. 1 shows this calculation for the parallel orientation, a coherence length of 3.3 a.u., and $\delta = 0$. It is in poor agreement with experiment. However, the same calculation with a phase

shift of $\delta = \pi$ is in excellent agreement up to scattering angles of about 1.2 mrad (except for $\theta_p < 0.1$ mrad, which is smaller than the angular resolution) for the coherent case (solid curve) and up to 1.0 mrad for the incoherent case (dashed curve). Between approximately 1.2 and 3.5 mrad the calculation reproduces the location of the oscillation extrema rather well; however, it systematically underestimates the magnitude of the FDCS. Only for angles larger than 3.5 mrad is the agreement between experiment and theory poor. We also note that theory agrees with experiment that even for the incoherent case a structure is visible in the FDCS, which is, however, weaker than in the coherent case. This reflects that the interference visibility does not abruptly drop to zero once the coherence length drops below the dimension of the diffracting object, but rather this is a smooth transition. (In fact, according to the van Zittert-Zernicke theorem the visibility reappears in an oscillatory manner, although with reduced amplitude, as the coherence length is further decreased).

In conclusion, we have measured FDCS for capture accompanied by dissociation through vibrational excitation. In the FDCS for fixed molecular orientations as a function of scattering angle we identified molecular two-center interference as well as single center interference. Our data are qualitatively consistent with a molecular eikonal calculation, which assumes a phase shift of π in the two-center interference term. However, the origin of this phase shift is currently not understood. Furthermore, at large scattering angles there are significant quantitative discrepancies between experiment and theory. Therefore, further theoretical studies are needed, which should treat two-center interference from first principles.

This work was supported by the National Science Foundation under Grant No. PHY-1401586, by Universidad Nacional de Cuyo (Argentina) under Grant No. 06/C480, and by the project ELI-Extreme Light Infrastructure-phase 2 (Project No. CZ.02.1.01/0.0/0.0/15_008/0000162) from the European Regional Development Fund.

[1] M. Schulz, R. Moshammer, D. Fischer, H. Kollmus, D. H. Madison, S. Jones, and J. Ullrich, Nature (London) **422**, 48 (2003).
[2] T. Rescigno, M. Baertschy, W. A. Isaacs, and C. E. McCurdy, Science **286**, 2474 (1999).
[3] A. Lahmann-Bennani, J. Phys. B **24**, 2401 (1991).
[4] M. Schulz and D. H. Madison, Int. J. Mod. Phys. A **21**, 3649 (2006).
[5] D. Madison, M. Schulz, S. Jones, M. Foster, R. Moshammer, and J. Ullrich, J. Phys. B **35**, 3297 (2002).
[6] M. McGovern, C. T. Whelan, and H. R. J. Walters, Phys. Rev. A **82**, 032702 (2010).
[7] K. A. Kouzakov, S. A. Zaytsev, Y. V. Popov, and M. Takahashi, Phys. Rev. A **86**, 032710 (2012).
[8] M. Foster, D. H. Madison, J. L. Peacher, M. Schulz, S. Jones, D. Fischer, R. Moshammer, and J. Ullrich, J. Phys. B **37**, 1565 (2004).
[9] M. F. Ciappina, W. R. Cravero, and M. Schulz, J. Phys. B **40**, 2577 (2007).
[10] A. K. Edwards, R. M. Wood, J. L. Davis, and R. L. Ezell, Phys. Rev. A **42**, 1367 (1990).
[11] L. Ph. H. Schmidt, S. Schössler, F. Afaneh, M. Schöffler, K. E. Stiebing, H. Schmidt-Böcking, and R. Dörner, Phys. Rev. Lett. **101**, 173202 (2008).
[12] L. Ph. H. Schmidt, T. Jahnke, A. Czasch, M. Schöffler, H. Schmidt-Böcking, and R. Dörner, Phys. Rev. Lett. **108**, 073202 (2012).
[13] H. T. Schmidt *et al.*, Phys. Rev. Lett. **101**, 083201 (2008).
[14] A. Senftleben, T. Pflüger, X. Ren, O. Al-Hagan, B. Najjari, D. Madison, A. Dorn, and J. Ullrich, J. Phys. B **43**, 081002 (2010).
[15] K. N. Egodapitiya, S. Sharma, A. Hasan, A. C. Laforge, D. H. Madison, R. Moshammer, and M. Schulz, Phys. Rev. Lett. **106**, 153202 (2011).
[16] S. Sharma, A. Hasan, K. N. Egodapitiya, T. P. Arthanayaka, G. Sakhelashvili, and M. Schulz, Phys. Rev. A **86**, 022706 (2012).
[17] S. Sharma, T. P. Arthanayaka, A. Hasan, B. R. Lamichhane, J. Remolina, A. Smith, and M. Schulz, Phys. Rev. A **90**, 052710 (2014).
[18] T. P. Arthanayaka, S. Sharma, B. R. Lamichhane, A. Hasan, J. Remolina, S. Gurung, and M. Schulz, J. Phys. B **48**, 071001 (2015).
[19] J. M. Feagin and L. Hargreaves, Phys. Rev. A **88**, 032705 (2013).
[20] L. Sarkadi, I. Fabre, F. Navarrete, and R. O. Barrachina, Phys. Rev. A **93**, 032702 (2016).
[21] C. Keller, J. Schmiedmayer, and A. Zeilinger, Opt. Commun. **179**, 129 (2000).
[22] X. Wang, K. Schneider, A. LaForge, A. Kelkar, M. Grieser, R. Moshammer, J. Ullrich, M. Schulz, and D. Fischer, J. Phys. B **45**, 211001 (2012).
[23] K. Schneider, M. Schulz, X. Wang, A. Kelkar, M. Grieser, C. Krantz, J. Ullrich, R. Moshammer, and D. Fischer, Phys. Rev. Lett. **110**, 113201 (2013).
[24] T. Arthanayaka, B. R. Lamichhane, A. Hasan, S. Gurung, J. Remolina, S. Borbély, F. Járai-Szabó, L. Nagy, and M. Schulz, J. Phys. B **49**, 13LT02 (2016).
[25] K. Gassert *et al.*, Phys. Rev. Lett. **116**, 073201 (2016).
[26] F. Navarrete, M. F. Ciappina, L. Sarkadi, and R. O. Barrachina, [Nucl. Instrum. Methods Phys. Res., Sect. B (to be published)].
[27] A. Igarashi and L. Gulyas, J. Phys. B **50**, 035201 (2017).
[28] M. Gudmundsson *et al.*, J. Phys. B **43**, 185209 (2010).
[29] T. E. Sharp, At. Data Nucl. Data Tables **2**, 119 (1970).
[30] See Supplemental Material at http://link.aps.org/supplemental/10.1103/PhysRevLett.119.083402 for plot of differential dissociative capture cross sections as a function of the molecular orientation relative to the projectile beam axis.
[31] S. F. Zhang, D. Fischer, M. Schulz, A. B. Voitkiv, A. Senftleben, A. Dorn, J. Ullrich, X. Ma, and R. Moshammer, Phys. Rev. Lett. **112**, 023201 (2014).
[32] K. Støchkel *et al.*, Phys. Rev. A **72**, 050703 (2005).
[33] E. Ghanbari-Adivi and S. H. Sattarpour, Mol. Phys. **113**, 3336 (2015).
[34] M. F. Ciappina and R. D. Rivarola, J. Phys. B **41**, 015203 (2008).